New Phytologist

Research

An R2R3-MYB transcription factor represses the transformation of α- and β-branch carotenoids by negatively regulating expression of *CrBCH2* and *CrNCED5* in flavedo of *Citrus reticulate*

Feng Zhu[1,2,3], Tao Luo[1,2,3], Chaoyang Liu[1,2,3], Yang Wang[1,2,3], Hongbin Yang[1,2,3], Wei Yang[1,2,3], Li Zheng[1,2,3], Xue Xiao[1,2,3], Mingfei Zhang[1,2,3], Rangwei Xu[1,2,3], Jianguo Xu[4], Yunliu Zeng[1,2,3], Juan Xu[1,2,3], Qiang Xu[1,2,3], Wenwu Guo[1,2,3], Robert M. Larkin[1,2,3], Xiuxin Deng[1,2,3] and Yunjiang Cheng[1,2,3]

[1]Key Laboratory of Horticultural Plant Biology, Ministry of Education, Huazhong Agricultural University, Wuhan, Hubei 430070, China; [2]Key Laboratory of Horticultural Crop Biology and Genetic improvement (Central Region), Ministry of Agriculture, Huazhong Agricultural University, Wuhan, Hubei 430070, China; [3]The Institute of Citrus Science, Huazhong Agricultural University, Wuhan, Hubei 430070, China; [4]Zhejiang Citrus Research Institute, Taizhou, Zhejiang 318020, China

Author for correspondence:
Yunjiang Cheng
Tel: +86 2787281796
Email: yjcheng@mail.hzau.edu.cn

Received: *16 February 2017*
Accepted: *30 May 2017*

New Phytologist (2017)
doi: 10.1111/nph.14684

Key words: ABA, carotenoid metabolism, *Citrus reticulata*, fruit development and postharvest, MYB transcription factor, transcriptional regulation.

Summary

- Although the functions of carotenogenic genes are well documented, little is known about the mechanisms that regulate their expression, especially those genes involved in α - and β-branch carotenoid metabolism.
- In this study, an R2R3-MYB transcriptional factor (CrMYB68) that directly regulates the transformation of α- and β-branch carotenoids was identified using Green Ougan (MT), a stay-green mutant of *Citrus reticulata* cv *Suavissima*. A comprehensive analysis of developing and harvested fruits indicated that reduced expression of *β-carotene hydroxylases 2* (*CrBCH2*) and *9-cis-epoxycarotenoid dioxygenase 5* (*CrNCED5*) was responsible for the delay in the transformation of α- and β-carotene and the biosynthesis of ABA. Additionally, the expression of these genes was negatively correlated with the expression of *CrMYB68* in MT.
- Further, electrophoretic mobility shift assays (EMSAs) and dual luciferase assays indicated that CrMYB68 can directly and negatively regulate *CrBCH2* and *CrNCED5*. Moreover, transient overexpression experiments using leaves of *Nicotiana benthamiana* indicated that CrMYB68 can also negatively regulate *NbBCH2* and *NbNCED5*.
- To overcome the difficulty of transgenic validation, we quantified the concentrations of carotenoids and ABA, and gene expression in a revertant of MT. The results of these experiments provide more evidence that CrMYB68 is an important regulator of carotenoid metabolism.

Introduction

Carotenoids are indispensable components of primary metabolism in plants and also contribute much to the color and nutritional quality of agricultural products (Zechmeister & Polgar, 1941; Demmigadams *et al.*, 1995; Lewinsohn *et al.*, 2005; Cazzonelli, 2011; Zhang *et al.*, 2015, 2017). In higher plants, carotenoid biosynthesis is divided into two parts: the early steps that yield lycopene and the subsequent branches that produce both α- and β-carotene and xanthophylls derived from α- and β-carotene. Phytoene synthase (PSY) converts two molecules of the C20-precursor geranylgeranyl pyrophosphate (GGPP) to phytoene. Subsequently, two desaturases (phytoene desaturase and ζ-carotene desaturase) and two isomerases (ζ-carotene isomerase and carotene isomerase) catalyze the biosynthesis of lycopene from phytoene. Two distinct pathways cyclize lycopene on both ends, yielding α- and β-carotene. Hydroxylation of both α- and β-carotene and the subsequent epoxidation of particular xanthophylls result in a variety of xanthophylls (Sun *et al.*, 1996; Shewmaker *et al.*, 1999; Cazzonelli, 2011). β-Carotene hydroxylases (BCHs) are key enzymes in the biosynthesis of xanthophylls from both α - and β-carotene. Indeed, the ectopic expression of *BCHs* disrupts the balance of carotenes and xanthophylls and affects the total accumulation of carotenoids (Tian *et al.*, 2004; Diretto *et al.*, 2007; Arango *et al.*, 2014). Two xanthophylls produced by the β-carotene branch, violaxanthin and neoxanthin, are transformed by 9-*cis*-epoxycarotenoid dioxygenases (NCEDs) and several other enzymes to yield ABA (Finkelstein, 2013). As the main

steps of carotenogenesis have been thoroughly illustrated, the transcriptional regulation of the pathway is becoming a new focus in carotenoid metabolism research.

Recently, the suppression of several regulatory factors, such as *DE-ETIOLATED1* (*DET1*) and *Ethylene Response Factor 6* (*ERF6*), was demonstrated to significantly increase the carotenoid content in tomato fruits (Davuluri *et al.*, 2005; Lee *et al.*, 2012). Loss-of-function mutations in two R2R3-MYB transcription factors (TFs) (*RCP1* in *Mimulus lewisii* and *NlMYB305* in *Nicotiana langsdorffii* × *N. sanderae*) reduced the accumulation of carotenoids in floral nectar guides (Liu *et al.*, 2009; Sagawa *et al.*, 2016). However, it is possible that the suppression of DET1 and ERF6 affects carotenoid metabolism by indirect mechanisms because ERF6 and DET1 contribute to other aspects of the ripening process and light-regulated development, and little is known about the direct transcriptional regulation of the genes that encode carotenoid biosynthetic enzymes. TFs are effective regulators of metabolism, and carotenoids contribute significantly to a number of important processes (e.g. photosynthesis and biosynthesis of vital regulators, such as ABA and strigolactones). Thus, mutations in the TFs that directly regulate carotenoid metabolism may induce lethality. Consistent with this notion, few TFs have been reported to directly regulate carotenoid metabolism. During seedling development in *Arabidopsis thaliana*, phytochrome-interacting factor 1 (PIF1) was reported to directly repress the expression of the *PSY* gene (Toledoortiz *et al.*, 2010). Moreover, a MADS-box TF named RIPENING INHIBITOR (RIN) in *Solanum lycopersicum* and a NAM/ATAF1/2/CUC2 (NAC) TF named CpNAC1 in *Carica papaya* L. were reported to directly induce the expression of *SlPSY* and *CpPDS2/4*, respectively (Martel *et al.*, 2011; Fu *et al.*, 2016). All of these TFs regulate lycopene biosynthesis, while the TFs that directly regulate the α- and β-branches of carotenoid metabolism remain unknown.

Citrus, one of the most important fresh fruit crops, accumulates various carotenoids to high concentrations (Kato *et al.*, 2004). In recent decades, the carotenoids that accumulate in citrus pericarp (flavedo) and pulp have been well documented (Rodrigo *et al.*, 2004, 2013; Liu *et al.*, 2007; Luo *et al.*, 2015). Moreover, some researchers have reported that carotenoid metabolism in citrus is highly regulated by the coordinated expression of carotenogenic genes (Rodrigo *et al.*, 2004; Liu *et al.*, 2007; Xu *et al.*, 2009; Luo *et al.*, 2015). However, because of the lack of suitable research materials in citrus, the mechanisms that regulate the expression of carotenogenic genes remain largely unknown.

In the present study, we report on a stay-green mutant of *Citrus reticulata* cv *Suavissima* named Green Ougan (MT), which was discovered in 2000 in an orchard of Wenzhou (Zhejiang Province, China). Fortunately, in 2013, we found one revertant branch (MT-WT) on an MT tree that exhibited the same phenotype as the original wild-type Ougan (WT). Previous research on the color formation in citrus flavedo indicated that chlorophyll (Chl) catabolism largely determines the colors of the flavedo (either orange or brown) (Alos *et al.*, 2008; Rodrigo *et al.*, 2013). Considering the important roles of carotenoids in the protection of photosystems and the color formation of fruits, we infer that carotenoid metabolism may also influence the stay-green phenotype of MT. In the present study, we report that the transformation of α- and β- branch carotenoids was indeed delayed in MT and that an MYB TF (CrMYB68) can repress the transformation of α- and β-branch carotenoids by directly suppressing the expression of *CrBCH2* and *CrNCED5*.

Materials and Methods

Plant materials and sampling strategies

Green Ougan (MT), a spontaneous stay-green mutant of the commercial variety Ougan (WT) (*Citrus reticulata* cv *Suavissima*), was initially found in 2000 in an orchard in Wenzhou City (Zhejiang Province, China). MT was propagated by grafting onto different rootstocks. The mutant phenotype was stable from 2005 to 2010. The phenological period of MT tree was identical to that of WT trees.

To comprehensively analyze the differences between WT and MT, fruit samples were harvested at 110, 170, 210 d after flowering (DAF) and 30 d after storage (DAS) in 2011 and 2013. Fruits at the breaking stage (185 DAF) were also collected in 2013. Fruits of each genotype at each stage were collected from three different trees, with 30 representative fruits from each tree. The flavedo of 10 fruits was separately and immediately frozen in liquid nitrogen, and stored at −80°C until analysis. Other fruits were used for fruit quality analysis. At 210 DAF, 50 more fruits from each tree were stored for 30 d at the optimum cold storage temperature (15–18°C) and relative humidity (75–85%). The fruits were then collected and stored at −80°C until analysis.

In the autumn of 2013, after a careful survey of the phenotypes of the MT trees in the orchard, a revertant (MT-WT) was found on one branch of one MT tree. The phenotype of MT-WT fruits was indistinguishable from that of WT fruits, and the revertant phenotype was stable in the following years. The fruits on the revertant branch were divided into three groups based on their location on the sub-branch, and were collected at 240 DAF in 2013 and at 210 DAF in 2015. In 2014, the quantities of these fruits were not sufficient for our experiments because of the alternate bearing of the tree.

Determination of fruit properties and Chl and carotenoid contents

The color index (CI) and total Chl were quantified as described previously (Yin *et al.*, 2016). Firmness, total soluble solid (TSS) and rotting rate were measured as described previously (Zhu *et al.*, 2016). Titratable acid (TA) was measured using digital acidity meters (GMK-835; G-Won Hitech Co. Ltd, Seoul, Korea) following the manufacturer's instructions (Obenland *et al.*, 2011). The maturity index was the ratio of TSS/TA. The carotenoid content was quantified using reverse-phase high-performance liquid chromatography (RP-HPLC) as described by Liu *et al.* (2007).

Quantitation of ABA content in the two genotypes

Abscisic acit was extracted from the citrus flavedo from the fruits harvested in 2011 as recommended by Wang *et al.* (2016a,b). Briefly, 0.2 g of ground sample was added to 750 µl of extraction buffer containing methanol : H_2O : acetic acid (80 : 19 : 1, v/v/v) in a 2 ml tube. After shaking at a speed of 140 rpm overnight at 4°C, the sample was centrifuged at 12 000 ***g*** for 15 min. The upper phase was transferred to a new 1.5 ml tube. A total of 400 µl of extraction buffer was added to the remainder of the precipitate, followed by shaking for 4 h at 4°C and centrifugation at 12 000 ***g*** for 15 min. The combined extracts were dried under a stream of nitrogen gas. An internal standard for ABA content was prepared and ABA content was analyzed according to Ma *et al.* (2014) using an HPLC system equipped with an electrospray ionization mass spectrometer (ESI–MS) (HPLC; API3000 mass spectrometer, Agilent 1100; Agilent Technologies, Palo Alto, CA, USA). To independently quantify the concentrations of ABA in MT, MT-WT and WT from the samples collected in 2013 and 2015, ABA was extracted using an 80% methanol solution, and ABA concentrations were quantified using the enzyme-linked immunosorbant assay (ELISA) method, as described previously (Yang *et al.*, 2001; Wang *et al.*, 2012). Analysis of the ELISA data was performed as described by Weiler *et al.* (1981).

RNA isolation and transcriptome profile analyses

All RNA samples were isolated as described by Liu *et al.* (2007). Two biological replicates of RNA from the flavedo of WT and MT collected at 170 DAF in 2011 were hybridized to the GeneChip Citrus Genome Arrays (Affymetrix, Santa Clara, CA, USA). The three biological replicates at 210 DAF and 30 DAS from the two genotypes collected in 2011 were analyzed using digital gene expression profiling. We used the procedures described by Ma *et al.* (2014) for gene annotation and analysis of differentially expressed genes. Transcriptome datasets generated using the GeneChip Citrus Genome Array platform and digital gene expression profiling can be found in the Gene Expression Omnibus (GEO) with the accession numbers GSE94689 and GSE94810, respectively.

After the total RNA was extracted from the citrus samples, single-strand cDNA was synthesized using the RevertAid First Strand cDNA Synthesis Kit (Fermentas, Burlington, Canada). Primers were designed using Primer Express (Applied Biosystems, Foster City, CA, USA). The gene-specific primers used for real-time quantitative reverse transcription polymerase chain reaction (qRT-PCR) are presented in Supporting Information Table S1. Real-time qRT-PCR was performed using 384-well plates, the ABI 7900 Fast Real Time System (PE; Applied Biosystems, Foster City, CA, USA), and the Roche LightCycler 480II System (Roche Diagnostics). The qRT-PCR data were analyzed using the $2^{-\Delta\Delta Ct}$ analysis method according to Bustin *et al.* (2009).

Isolation of *CrMYB68*, *CrBCH2* and *CrNCED5* and sequence analysis of CrMYB68

The full-length sequences of *CrMYB68*, *CrBCH2* and *CrNCED5* were obtained from the cDNA and DNA of WT and MT. The primers are listed in Table S1. Different amino acid sequences were aligned and edited using the ClustalW program and GeneDoc software. The phylogenetic tree was generated using CrMYB68 and 126 MYB amino acid sequences from *A. thaliana* using Mega 5.0 with the neighbor-joining algorithm (Tamura *et al.*, 2011). The respective name, synonym, and The Arabidopsis Information Resource ID of the 126 MYB sequences are presented in Table S2. Bootstrap analysis was performed using 1000 replicates in Mega to evaluate the reliability of different phylogenetic group assignments.

Subcellular localization of CrMYB68

Subcellular localization of the CrMYB68 protein was performed using citrus mesophyll protoplasts (HB pummelo, *Citrus grandis* L. Osbeck) as recommended by Liu *et al.* (2016). The *35S:CrMYB68–GFP* fusion construct was produced by inserting the coding sequence from CrMYB68 without a stop codon into the pM999-35 vector (provided by Dr Wei Zong and Dr Lizhong Xiong). The *35S:OsGhd7–CFP* transgene was used to produce the nuclear maker (Liu *et al.*, 2016). The florescence images were acquired using a confocal laser-scanning microscope (TCS SP2; Leica, Wetzlar, Germany). For imaging, green fluorescent protein (GFP) and cyan fluorescent protein (CFP) were excited using an Argon laser at 488 nm and 430 nm wavelengths, respectively. The emission filters were 500–530 nm for GFP and 470–510 nm for CFP. Chl autofluorescence was monitored using either 488 or 514 nm excitation wavelengths, and 650–750 nm detection windows.

Protein preparation, identification, and the SAAB assay

The coding sequence of *CrMYB68* was subcloned into pET15 (Novagen, Darmstadt, Germany). The resulting plasmid expressed a recombinant CrMYB68 protein with a 6-His tag fused to the N-terminus. This pET15-*CrMYB68* vector was introduced into the *Escherichia coli* strain BL21 (DE3). The His-tagged protein was purified using the method of Shen *et al.* (2016). The most abundant band in the gel was identified as the CrMYB68 protein using the matrix-assisted laser desorption ionization-time of flight (MALDI-TOF)/time of flight mass spectrometry (TOF MS) method (Yan *et al.*, 2000). To analyze the consensus DNA-binding sequence of the protein, selected amplification and binding (SAAB) assay was performed using the method of Weng *et al.* (2015).

Electrophoretic mobility shift assay

The electrophoretic mobility shift (EMSA) assay was conducted as described previously (Liu *et al.*, 2016; Zong *et al.*, 2016) with some modifications. Briefly, the His-fused CrMYB68 was

expressed and purified as described earlier. The 5′ FAM-labeled oligonucleotide probes were directly synthesized and labeled by the Shanghai Sangon Company (Shanghai, China). To perform binding reactions, the binding solution (0.1% Nonidet P-40, 1 mM benzamidine, 0.5 mM phenylmethylsulfonyl fluoride, 0.5 mM dithiothreitol, 50 μg ml^{-1} BSA and 100 ng μl^{-1} poly (dI-dC)), purified His-fused CrMYB68 and 1 μl of the 5′ FAM labeled probe (10 μmol l^{-1}) were mixed together and incubated at 4°C for 45 min. For the competition assays, the nonlabeled probe was incubated with protein and binding buffer at 4°C for 45 min. Next, 1 μl of the 5′-FAM-labeled probe (10 μmol l^{-1}) was added and incubated at 4°C for 45 min. The samples were loaded onto a prerun 6% polyacrylamide gel. Electrophoresis was performed at 4°C using 0.5× Tris-Borate-EDTA as the electrophoresis buffer in the dark for 1 h. Gel images were acquired using the Amersham Imager 600 (GE Healthcare, Tokyo, Japan).

Dual luciferase transcriptional activity assay

Owing to the high stability, transformation efficiency and short growth cycle, the dual luciferase transcriptional activity assay was conducted using rice protoplasts as described previously (Zong *et al.*, 2016). The rice sheath strips from 14-d-old seedlings of ZH11 (*Oryza sativa spp.* japonica) were treated with digestion solution (10 mM MES, pH 5.7, 0.6 M mannitol, 1 mM $CaCl_2$, 5 mM β-mercaptoethanol, 0.1% BSA, 0.3% cellulase RS, and 0.75% Macerozume R10) for 4 h. After filtering through a nylon mesh (35 μm), the protoplasts were collected and incubated in W5 solution (154 mM NaCl, 125 mM $CaCl_2$, 5 mM KCl, and 2 mM MES, pH 5.7) at room temperature (25°C) for 1.5 h, collected by centrifugation at 100 ***g*** for 8 min, and finally resuspended in MMG solution (0.6 M mannitol, 4 mM MES (pH 5.7), and 15 mM $MgCl_2$). For transformation, 3 μg of each plasmid was gently mixed with 100 μl of protoplasts and 110 μl of polyethylene glycol-$CaCl_2$ solution. The mixture was incubated at room temperature for 15 min in the dark. The transformed protoplasts were incubated in 24-well culture plates for 12 h. The Dual-Luciferase Reporter Assay System (Promega) was used to measure the luciferase activity following the manufacturer's instructions. 'None' (empty vector) was used as the effector, '35S-GAL4-fLUC' was used as the reporter, and *AtUbi*::rLUC was used as an internal control. Three independent transformations for each sample were performed. The relative luciferase activity was calculated as the ratio of fLUC/rLUC. All of the plasmids used in this assay were purified using the Qiagen Plasmid Midi Kit.

Infiltration of tobacco with agrobacterium

Nicotiana benthamiana was grown in an environmentally controlled chamber at 24°C and received cycles of 14 : 10 h, light : dark. Agrobacterium infiltration was conducted as described previously (Hellens *et al.*, 2005). Total RNA was extracted from tobacco leaves using the RNAiso Plus (Takara, Dalian, China) Kit according to the manufacturer's instructions. qRT-PCR experiments and ABA measurements (using the ELISA method) were conducted as described for the citrus sample. The gene encoding the 60S ribosomal protein *L23* from *N. benthamiana* was used as the reference gene (Liu *et al.*, 2012).

Accession numbers

The sequence data for *NbBCH2* (Niben101Scf01232g) and *NbNCED5* (Niben101Scf00897g) can be found in the Sol Genomics Network (https://solgenomics.net/). AtMYB4, NP_195574.1; AtMYB6, NP_192684.1; *CrMYB68* (coding sequence, KY612511; promoter sequence, KY612514); *CrBCH2* (coding sequence, KY612512; promoter sequence, KY612515); and *CrNCED5* (coding sequence, KY612513; promoter sequence, KY612516) can be found at NCBI with the indicated accession numbers.

Results

Analysis of carotenoid pathway metabolites in MT and WT

During the development and harvested periods, MT fruits exhibited a stay-green phenotype. The CI (1000 a l^{-1} b^{-1}) of MT fruits was significantly lower than that of WT fruits (Fig. 1a). The maturity index (TSS/TA), firmness, and rotting rate during storage were also different between the two genotypes (Fig. S1). To understand the molecular basis of the stay-green phenotype of MT fruits, we analyzed the pigments of the flavedo from both genotypes. The results indicated that in MT flavedo, the degradation of Chl was significantly delayed (Fig. 1b). We also observed significant differences in the concentrations of carotenoids, which possibly contributed to the different fruit colors of the two genotypes. We found that α- and β-carotene accumulated to significantly higher concentrations in MT than in WT, and that β-cryptoxanthin and zeaxanthin, which are produced downstream of β-carotene, had significantly lower accumulation in the flavedo of MT than in that of WT during different stages of fruit development (Figs 1c–e, S1). At 210 DAF, the flavedo of MT still displayed higher concentrations of α-carotene (7.96 ± 1.94 μg g^{-1} FW) and β-carotene (18.87 ± 5.17 μg g^{-1} FW) than the flavedo of the WT (α-carotene, 1.20 ± 0.40 μg g^{-1} FW; β-carotene, 4.41 ± 1.28 μg g^{-1} FW). By contrast, the concentration of zeaxanthin was lower in the flavedo of MT (1.69 ± 0.49 μg g^{-1} FW) than in the flavedo of WT (21.41 ± 6.06 μg g^{-1} FW). Furthermore, ABA, a downstream product of carotenoid metabolism, was lower in the flavedo of MT than in that of the WT, especially at 210 DAF (1.50 ± 0.24 μg g^{-1} FW in MT; 2.34 ± 0.45 μg g^{-1} FW in WT) (Figs 1f, S2). These results indicate that there were significant differences in the amount of pigments (especially the α- and β-branch carotenoids) and ABA between the two genotypes.

Transcriptome analyses of MT and WT

To evaluate the differentially expressed genes between the two genotypes, flavedos from the two genotypes collected at 170

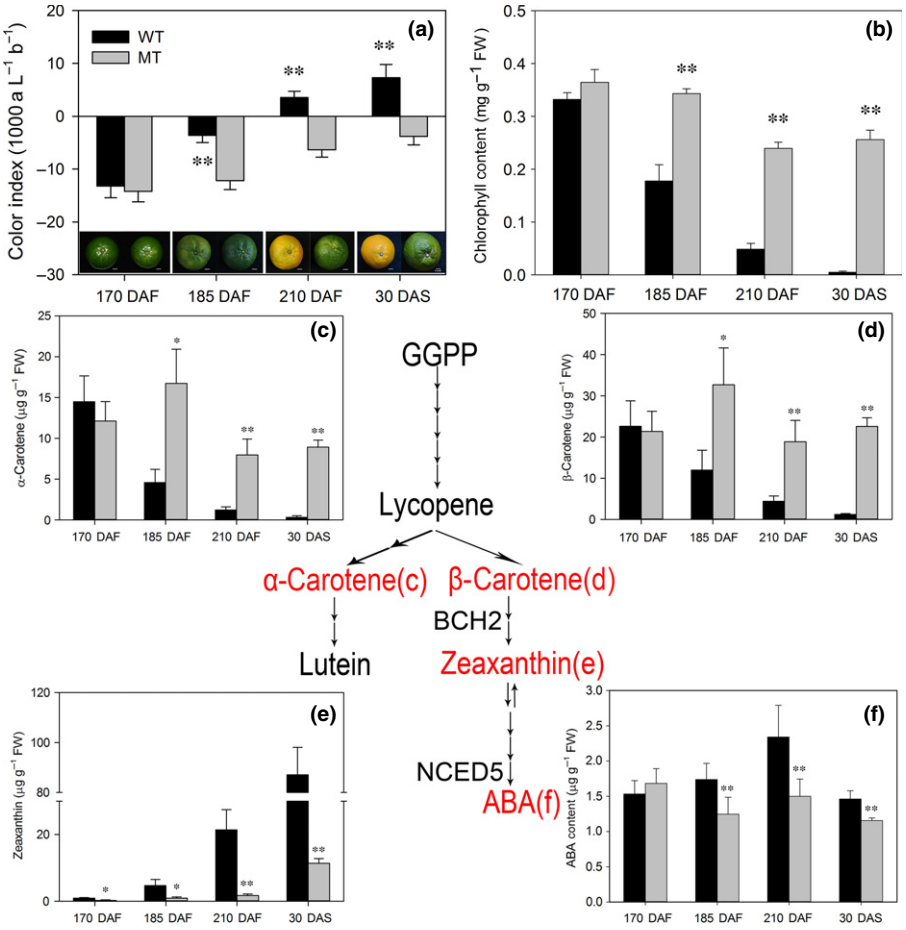

Fig. 1 Physiological and biochemical differences between Green Ougan (MT) and Ougan (WT) (*Citrus reticulata*) in 2013. (a) Flavedo color and color index, (b) total Chl, (c) α-carotene, (d) β-carotene, (e) zeaxanthin, and (f) ABA concentrations, were quantified in the flavedo. The values in each column are the means of three biological replicates. Error bars indicate SD. The asterisks indicate statistically significant differences determined by the Student's *t*-test: *, $P < 0.05$; **, $P < 0.01$. DAF, days after flowering; DAS, days after storage; GGPP, geranylgeranyl pyrophosphate.

DAF in 2011 were analyzed using the Citrus Genome Array (Affymetrix). We found that 383 (107 up and 276 down) probes showed significantly different expression levels between the two genotypes (Fig. S3; Table S3). In consideration of the quick development of Next Generation Sequencing and the *Citrus sinensis* Anotation Project (Xu *et al.*, 2013), Digital Gene Expression Profiling was used to comprehensively analyze the differentially expressed genes in the flavedos of the two genotypes collected at 210 DAF and at 30 DAS in 2011. We found that 1288 (504 up and 784 down) and 2408 (1338 up and 1070 down) genes were differentially expressed between the two genotypes, respectively (Fig. S3; Table S3).

To test whether particular functional categories of genes were differentially expressed in the two genotypes, the differentially expressed genes in each stage were annotated and divided into 35 MapMan catalogues (Table S3). At 170 DAF, 210 DAF and 30 DAS, we found two (cell wall and signaling), seven (cell wall, lipid metabolism, metal handling, hormone metabolism, nucleotide metabolism, protein, signaling) and 13 (photosynthesis, cell wall, lipid metabolism, metal handling, secondary metabolism, hormone metabolism, biodegradation of xenobiotics, misc, protein, signaling, transport, not assigned, mitochondrial electron transport/ATP synthesis) enriched catalogues, respectively, based on the Wilcoxon rank sum test in MapMan ($P < 0.05$) (Fig. 2a; Table S3). Thus, we expected to observe differences in these biological processes between these two genotypes.

A total of 82 genes were consistently differentially expressed at 170 DAF, 210 DAF and 30 DAS (Table S3). Interestingly, one of these genes, *CrNCED5*, was expressed at significantly lower levels in MT than in WT in all three stages. We observed five differentially expressed TFs in all three stages. There was a more than fourfold difference in the expression level of one of these TFs (*CrMYB68*) in all three stages (Table S3). Considering the significant differences in the concentrations of carotenoids and ABA between the two genotypes, the expression of the genes involved in these pathways was comprehensively analyzed at different stages of fruit development using the transcriptome data and qRT-PCR data at 110, 170, 185, and 210 DAF, and 30 DAS (Figs 2b, S4). It was found that *CrNCED5* and *CrBCH2*, which encode the enzymes that utilize α- and β-branch carotenoids as substrates, were significantly down-regulated in the flavedo of MT. Indeed, the expression of these two genes in MT was reduced by 23-fold and sixfold, respectively, relative to WT at 210 DAF (Fig. 2d,e). To analyze the functions of *CrNCED5* and *CrBCH2*, we transiently overexpressed *CrBCH2* and *CrNCED5* in tobacco leaves. It was found that the overexpression of *CrBCH2* and *CrNCED5* induced a remarkable degreening phenotype (accompanied by the reduction of α- and β-carotene) and the accumulation of ABA in tobacco leaves,

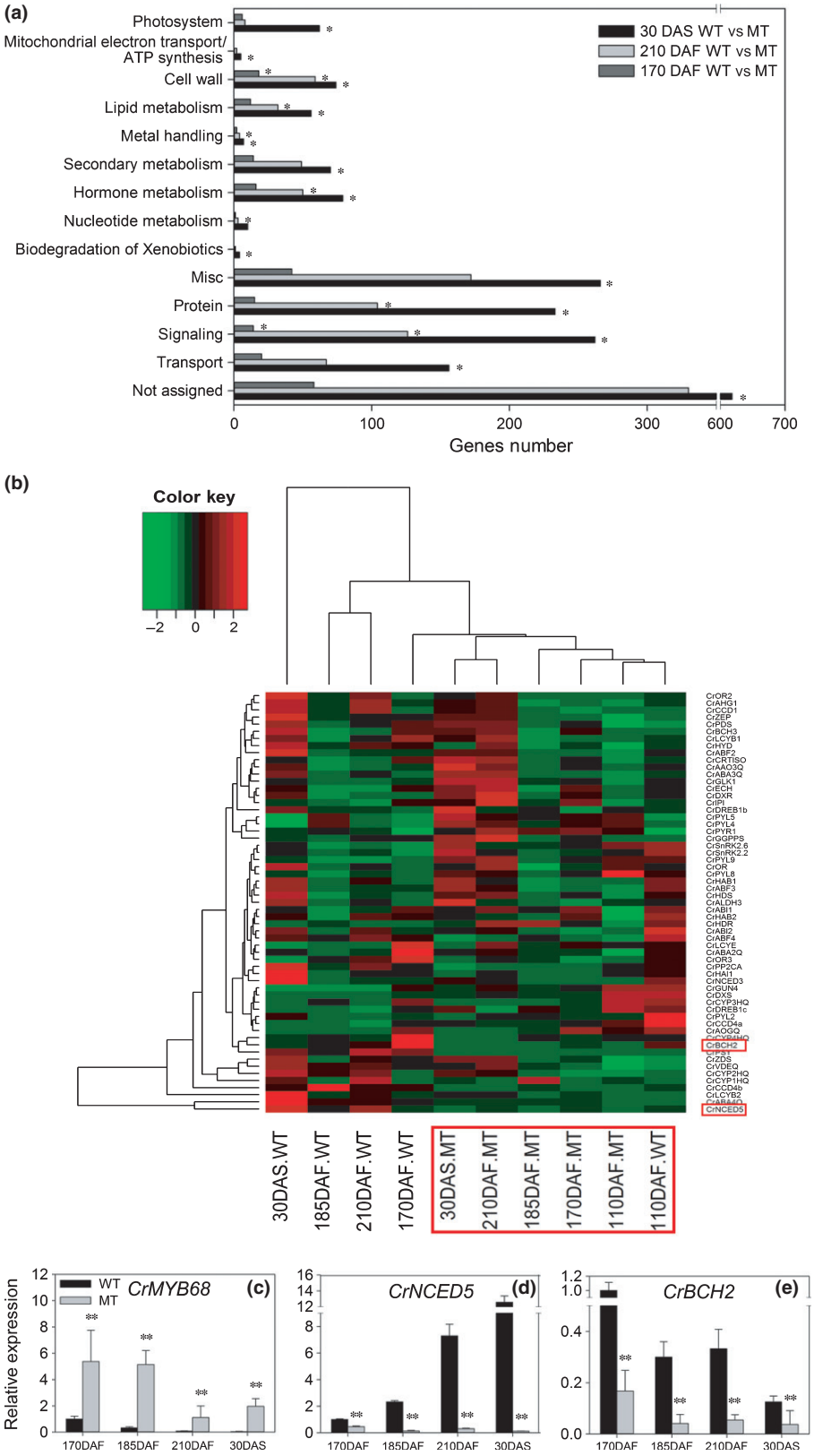

Fig. 2 Transcriptome differences in the two genotypes. (a) Distribution and functional categories of the differentially expressed genes at 170 and 210 d after flowering (DAF) and 30 d after storage (DAS) in 2011 based on MapMan. Asterisks indicate enriched catalogs (*, $P < 0.05$). (b) Cluster heat map based on the expression of 59 genes involved in carotenoid and ABA metabolism at 110, 170, 185 and 210 DAF and 30 DAS in 2013. The relative expression patterns of (c) *CrMYB68*, (d) *CrNCED5*, and (e) *CrBCH2* at 170, 185 and 210 DAF and at 30 DAS in 2013. The values in each column are the means of three biological replicates. Error bars indicate SD. The asterisks indicate statistically significant differences determined by Student's *t*-test: **, $P < 0.01$.

respectively (Fig. S5). We also found that the expression of *CrMYB68* was negatively correlated with the citrus ripening process and was higher in MT than in WT (Fig. 2c), indicating that CrMYB68 may act as a repressor of the citrus ripening process. Based on the phenotypic and gene expression data, the expression of *CrBCH2* and *CrNCED5* might explain the differences in the concentraions of α-carotene, β-carotene and ABA in the flavedos of MT and WT. We sequenced the promoters and coding

sequences from *CrBCH2*, *CrNCED5* and *CrMYB68* and found no differences between MT and WT (Table S4). Thus, we concluded that TFs, such as CrMYB68, may be responsible for the different expression levels of *CrBCH2* and *CrNCED5* in MT and WT.

Amino acid sequence alignment, subcellular localization and consensus DNA-binding sequence analysis of CrMYB68

Phylogenetic analysis of *A. thaliana* MYB proteins and CrMYB68 revealed that CrMYB68 clusters with AtMYB68 in the C20 subfamily (Liu *et al.*, 2014) (Fig. S6). In the *Citrus sinensis* Anotation Project (http://citrus.hzau.edu.cn/cgi-bin/orange/blast), this gene was annotated as TF RAX3, Myb-related protein MYB4, and transcription repressor MYB6. CrMYB68 is a protein containing 260 amino acid residues with a consensus sequence for an R2R3 domain in the N-terminus and a repressor C2-motif in the C-terminus (Fig. S7). Transient expression of a CrMYB68-GFP fusion protein in protoplasts demonstrated that CrMYB68-GFP accumulated in the nucleus (Fig. 3a), which is consistent with the fact that CrMYB68 serves as a TF. These results provide evidence that *CrMYB68* encodes a nuclear protein and may serve as a repressor of transcription.

The 6*HIS-CrMYB68 fusion protein was expressed in *E. coli* and then purified, yielding a protein with a mass of *c.* 35 kDa (Fig. 3c). Using the MALDI-TOF/TOF MS method, the most abundant band on the gel was identified as the CrMYB68 protein (Table S5). To determine the DNA-binding sequence of CrMYB68, the SAAB assay was performed. In the SAAB assay, the purified 6*HIS-CrMYB68 fusion protein was incubated with a synthetic random 14-mer oligonucleotide library. After six continuous rounds of selective incubation, we obtained 127 selected DNA fragments bound by CrMYB68 (Table S6), which were then subjected to Discriminative Regular Expression Motif Elicitation (DREME) analysis (Bailey, 2011). The DREME analysis indicated that among the 127 selected DNA fragments in the SAAB assay, CrMYB68 selected 58 fragments containing ACCTAC/GTAGGT, 43 fragments containing ACCAAC/GTTGGT, and 24 fragments containing AACAAC/GTTGTT (Fig. 3d). Based on these data, we concluded that CrMYB68 specifically binds these DNA sequences. These data are consistent with the previous finding that many R2R3-MYB TFs specifically bind AC elements (i.e. elements rich in adenosine and cytosine residues) (Gómez-Maldonado *et al.*, 2004).

CrMYB68 bound to the promoters of *CrBCH2* and *CrNCED5* and significantly inhibited their expression

We found an ACCAAC sequence (i.e. a CrMYB68 binding site) located between −306 and −300 bp upstream of the translational start codon in *CrBCH2* (Fig. 4a). To test whether CrMYB68 can bind to the promoter of *CrBCH2*, an EMSA was conducted using the 6*HIS-CrMYB68 fusion protein. We found that the purified 6*His-CrMYB68 protein could specifically bind to and retard the mobility of a 20 bp probe containing the ACCAAC motif from the promoter region of *CrBCH2*. By contrast, a mutant probe (AAAAAA) had almost no effect on the binding activity (Fig. 4b). To further test whether CrMYB68 regulates the expression of *CrBCH2*, a transient expression assay was performed using the luciferase system. For this experiment, we fused 1.5 kb of the *CrBCH2* promoter including the ACCAAC motif to the firefly luciferase reporter gene. The results indicated that CrMYB68 significantly repressed the activity of the 1.5 kb *CrBCH2* promoter (Fig. 4d), which is consistent with the prediction that CrMYB68 contains a transcription repressor domain (Fig. S7).

We found an AC-rich sequence (ACCAAA), which is similar to the sequence that we obtained in the SAAB assay, located between −42 and −36 bp upstream of the translational start codon in *CrNCED5* (Fig. 4a). An EMSA assay revealed that CrMYB68 could directly and specifically bind to a 31 bp probe containing this ACCAAA motif of the promoter region of *CrNCED5* (Fig. 4b). Moreover, dual luciferase assays indicated that the activity of the *CrNCED5* promoter was significantly inhibited by CrMYB68 (Fig. 4d). Based on these results, we concluded that CrMYB68 can directly bind to the promoter of *CrBCH2* and *CrNCED5* and significantly repress the expression of *CrBCH2* and *CrNCED5*.

Phenotypes of transient overexpression of *CrMYB68* in tobacco leaves

Owing to the long juvenile phase of citrus, it is not practical to test the functions of *CrMYB68 in vivo* using RNAi or stable overexpression lines. Tobacco leaves are widely used as a transient expression system for testing gene function. Thus, *CrMYB68* was transiently overexpressed in tobacco leaves using agrobacterium-mediated transformation. We found that the transient overexpression of *CrMYB68* significantly repressed the expression of *NbBCH2* and *NbNCED5* in tobacco leaves (Fig. 5a). An analysis of the promoter sequences of *NbBCH5* and *NbNCED5* indicated that several ACCAAA sequences were present upstream of the translational start codon. An EMSA assay revealed that CrMYB68 could directly and specifically bind to these DNA sequences from the promoters of *NbBCH2* and *NbNCED5* (Fig. 5b).

Phenotypic characterization of MT and the revertant

Although testing of our conclusions was not practical in perennial woody fruit trees because of the long juvenile phase, high heterozygosity and difficulty in obtaining homozygous T_1 and T_2 generations, our discovery of a revertant (MT-WT) that developed a yellow pericarp allowed us to test our results *in vivo* (Fig. 6). The change in the maturity index and the degradation of Chl were normal in MT-WT in both 2013 and 2015 (Fig. 6a,b). Carotenoid assays indicated that MT accumulated more α-carotene and β-carotene than did MT-WT. Similar to WT, at the mature stage, MT-WT mostly accumulated xanthophylls (Fig. 6c). Additionally, the ABA concentration in MT was lower than that in MT-WT in both

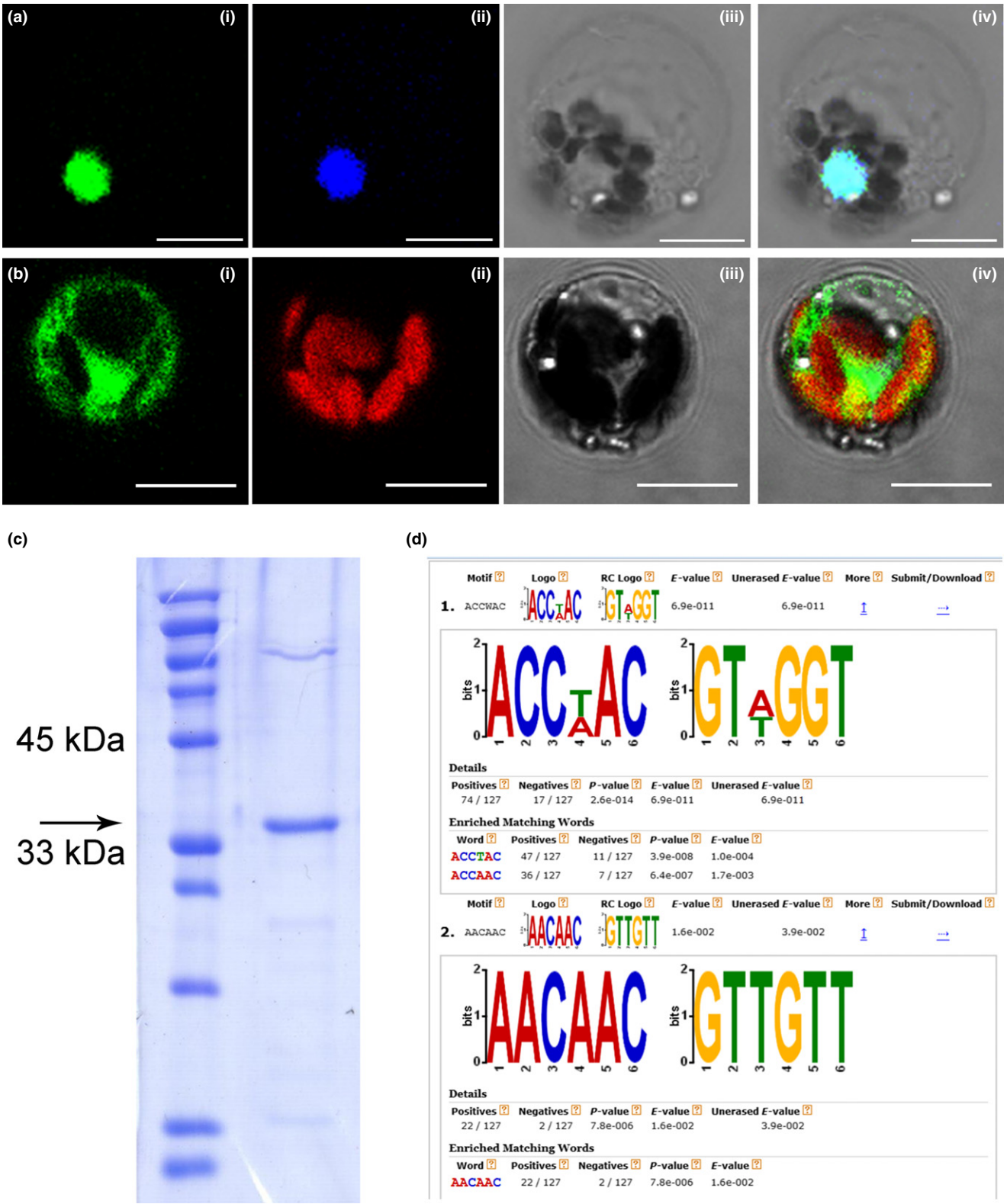

Fig. 3 Subcellular localization, prokaryotic expression, and consensus DNA binding sequence of CrMYB68. (a) Subcellular localization of *CrMYB68*-pM999. OsGhd7-CFP and CrMYB68-GFP were cotransformed into protoplasts. OsGhd7-CFP was used as a nuclear marker. (a, i) CrMYB68-GFP; (a, ii) OsGhd7-CFP; (a, iii) bright field; (a, iv) merged image. (b) Subcellular localization of pM-999 in protoplasts. (b, i) pM999-GFP; (b; ii) Chl fluorescence; (b; iii) bright field; (b; iv) merged image. Bars, 10 μm. (c) Prokaryotic expression analysis of His-tagged CrMYB68 on a Coomassie blue-stained 12% sodium dodecyl sulfate gel. (d) Consensus DNA-binding sequence of CrMYB68 obtained from the selected amplification and binding (SAAB) assay.

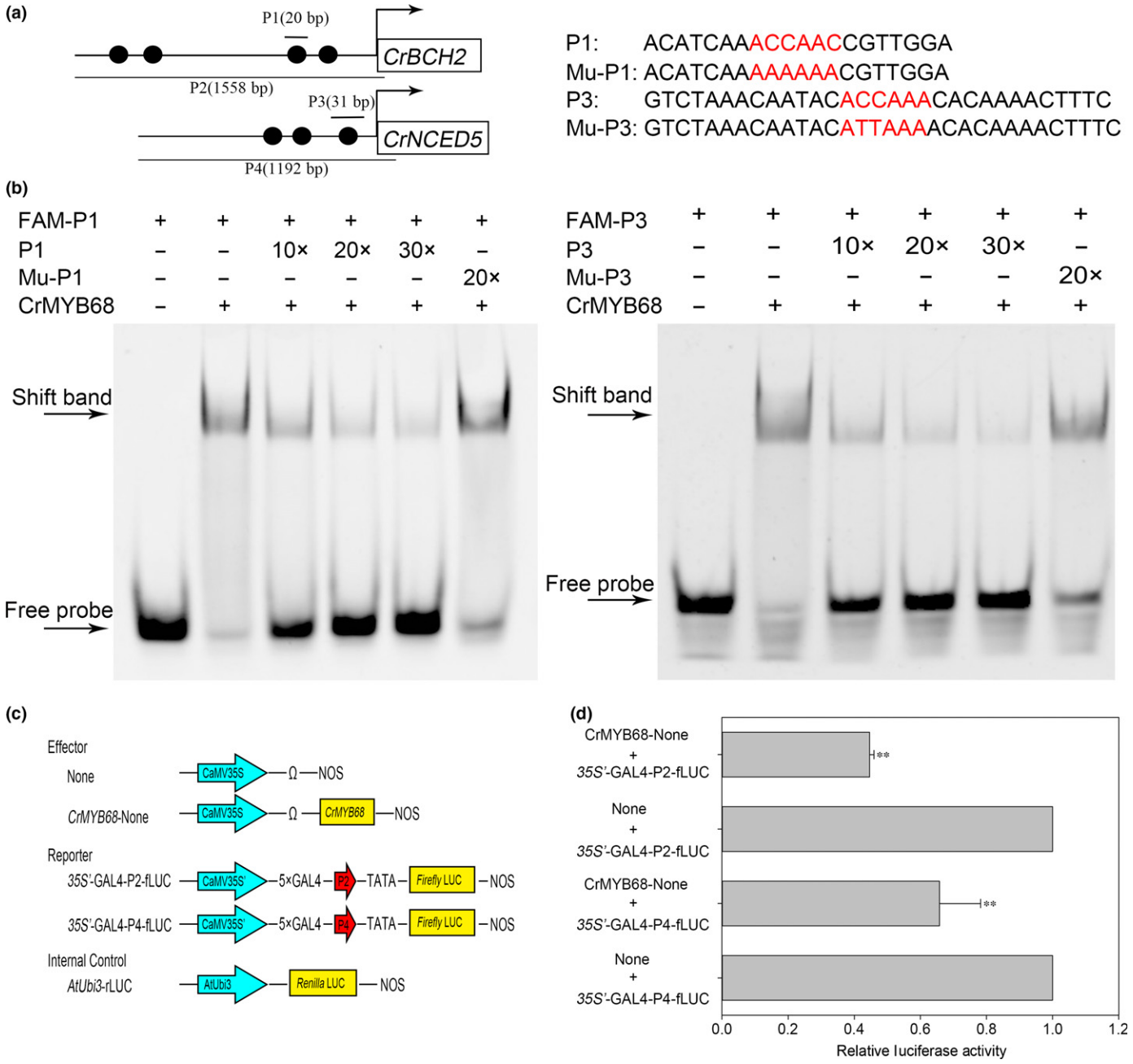

Fig. 4 Electrophoretic mobility shift assays (EMSAs) and dual luciferase assay. (a) Schematics of the promoter model and sequences used in the EMSA and dual luciferase assay (left). Sequences used in the EMSA (right). (b) EMSA showing the binding of CrMYB68 to the promoters of *CrBCH2* and *CrNCED5*. Ten-, 20-, and 30-fold excess of nonlabeled probes and 20-fold excess of mutant probes were used for competition. (c) Scheme of the constructs used in the dual luciferase assays. (d) CrMYB68 repressed the expression of *CrBCH2* and *CrNCED5*. The ratio of fLUC/rLUC represents the relative activity of the *CrBCH2* and *CrNCED5* promoters. P2 and P4 represented the promoter fragment of *CrBCH2* and *CrNCED5*, respectively, as shown in (a). The values in each column are the means of three biological replicates. Error bars indicate the SD. The asterisks indicate statistically significant differences determined by the Student's *t*-test: **, $P < 0.01$.

2013 and 2015 (Fig. 6e). Moreover, our qRT-PCR analysis indicated that the expression of *CrMYB68* was lower, and that of *CrBCH2* and *CrNCED5* was higher, in MT-WT than in MT (Fig. 6f). Based on these results and the differences observed between WT and MT, we concluded that CrMYB68 regulates carotenoid metabolism by regulating the expression of *CrBCH2* and *CrNCED5*.

Discussion

Although carotenoids play vital roles in various biological processes, little is known about the transcriptional regulation of the genes that encode carotenoid biosynthetic enzymes. Here, we used Ougan, Green Ougan and a revertant of Green Ougan to demonstrate that an R2R3-MYB transcriptional factor (CrMYB68)

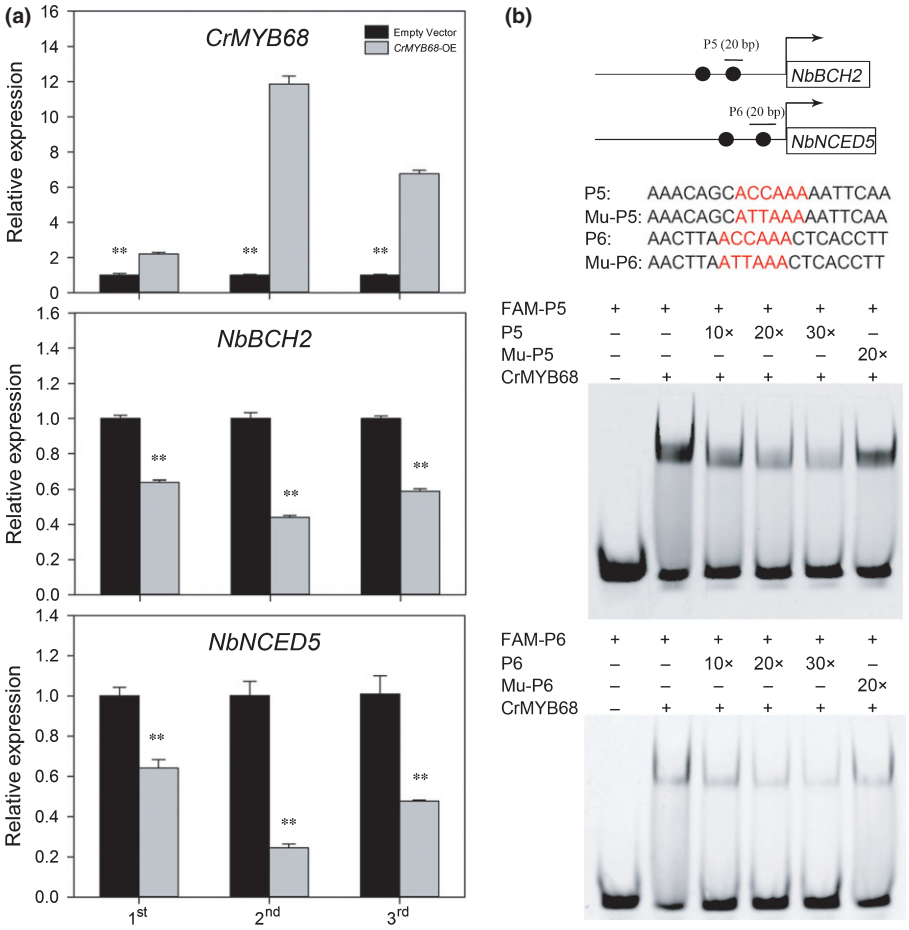

Fig. 5 Transient overexpression of *CrMYB68* in tobacco leaves. (a) Expression of *CrMYB68*, *NbBCH2*, and *NbNCED5* in tobacco leaves overexpressing *CrMYB68* and leaves infiltrated with the empty vector control. (b) Electrophoretic mobility shift assays (EMSA) showing the binding of CrMYB68 to the promoters of *NbBCH2* and *NbNCED5*. The upper panel contains a schematic diagram of the promoter models and sequences used in EMSA of *NbBCH2* and *NbNCED5*. The middle panel contains the wild-type and mutant sequences used in the EMSA of *NbBCH2* and *NbNCED5*. The lower panel shows the 10-, 20-, and 30-fold excess of nonlabeled probes and the 20-fold excess of mutant probes that were used for competition experiments to test the binding specificity. All transient overexpression experiments were conducted three times. The values in each column are the mean values from three replicates. Error bars indicate the SD. The asterisks indicate statistically significant difference determined by Student's *t*-test: **, $P < 0.01$.

directly regulates carotenoid metabolism. We conclude that CrMYB68 directly represses the transformation of α- and β-carotene by regulating the expression of *CrBCH2*, and indirectly influences carotenoid metabolism by regulating the expression of *CrNCED5*, which contributes to the biosynthesis of ABA.

CrMYB68 influences the transformation of α- and β-carotene

Both primary metabolism (e.g. photosynthesis) and vital regulatory mechanisms (e.g. signaling activated by ABA and strigolactones) are dependent on carotenoid metabolism. Thus, deficiencies in regulators of carotenoid metabolism might lead to lethality. Additionally, genetic redundancies among some key regulators, such as TFs, may limit the success of genetic approaches aimed at understanding the regulators of carotenoid metabolism in *A. thaliana*. However, plants do not depend on the carotenoids that accumulate in their fruits for survival. Moreover, distinct regulatory mechanisms may be responsible for the high accumulation of various carotenoids in fruits compared with other organs. Thus, fruits provide an excellent model system for studying the regulation of carotenoid metabolism.

During the early stages of development, the chloroplasts of fruits accumulate high concentrations of α- carotene, β-carotene and xanthophylls. These carotenoids play vital roles in preventing the oxidative damage of the photosystems (Searle & Wessels, 1978; Telfer, 2005; Cazzaniga *et al.*, 2012). When the ripening process is initiated or the plants are exposed to stress, the photosystem is dissembled, Chl is degraded, and the concentrations of α- and β-carotene are reduced. This reduction in α- and β-carotene is catalyzed by BCH or a nonenzymatic pathway (Rodrigo *et al.*, 2003, 2004). Consistent with these findings in previous studies, we found that transient overexpression of *CrBCH2* dramatically promotes the degreening process in tobacco leaves, which may result from the accelerated transformation of α- and β-carotene catalyzed by CrBCH2 (Fig. S5). During the ripening process, the transformation of α- and β-carotene into xanthophylls was normally initiated in the flavedo of WT and MT-WT (Figs 1c–e, 6c), which is similar to what happens in other citrus species (Rodrigo *et al.*, 2003, 2004). However, in the flavedo of MT, the reduction and transformation of α- and β-carotene were significantly delayed (Figs 1c–e, 6c). Several genes have been identified to directly catalyze the transformation of α- and β-carotene in *A. thaliana* and citrus (Arango *et al.*, 2014; Ma *et al.*, 2016). Among the homologous genes in citrus, only *CrBCH2* was expressed at significantly lower levels in MT relative to both WT and MT-WT (Figs 2e, 6f). These data and the result that the transient overexpression of *CrBCH2* in tobacco leaves induced Chl deficiencies indicate that lower expression of *CrBCH2* is at least partially responsible for the delay of the

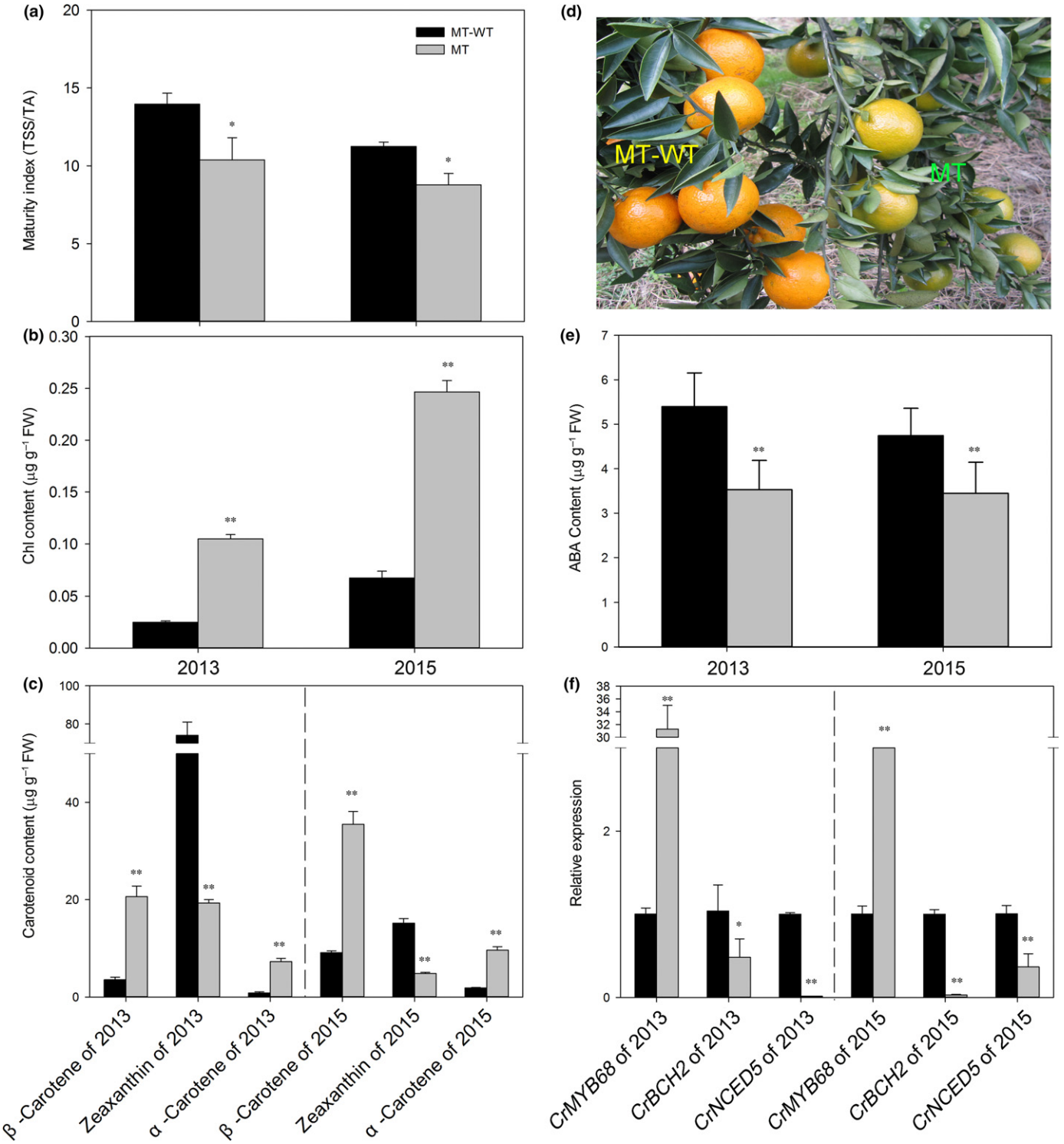

Fig. 6 Phenotypic characterization of Green Ougan (MT) and the revertant (*Citrus reticulata*) in different years. (a) The maturity index, (b) total Chl, (c) exhibited the content of different carotenoids (such as α-carotene, β-carotene and zeaxananthin) in the flavedo of MT and the revertant (MT-WT), (d) flavedo color on the tree at 240 d after flowering (DAF) in 2013, (e) endogenous ABA content, and (f) expression of *CrMYB68*, *CrBCH2*, and *CrNCED5* in the flavedo of MT and the revertant (MT-WT), were measured in different years. The samples were collected at 240 DAF in 2013 and at 210 DAF in 2015. The values in each column are the means of three biological replicates. Error bars indicate the SD. The asterisks indicate statistically significant differences determined by Student's *t*-test: *, $P < 0.05$; **, $P < 0.01$.

transformation of α- and β-carotene in the flavedo of MT. We conclude that the differences in the expression level of *CrBCH2* between MT and WT are probably caused by differences in the regulation of *CrBCH2*, because we found that the sequences of *CrBCH2*, including both the promoter and coding sequence, were identical in MT and WT.

To date, only a few TFs, such as *PIF1*, *RIN*, and *CpNAC1*, are known to regulate the expression of genes that encode carotenoid biosynthetic enzymes. All these TFs regulate the expression of the genes that contribute only to the early steps of lycopene biosynthesis. The TFs that directly regulate the expression of genes responsible for the transformation of α- and β-branch carotenoids remain unknown (Toledoortiz *et al.*, 2010; Martel *et al.*, 2011; Fu *et al.*, 2016). In MT, we observed an inverse correlation in the expression of *CrMYB68* and *CrBCH2* (Fig. 2c,e). The sequence analysis suggested that CrMYB68 might be a transcriptional repressor (Fig. S7). Additionally, the homolog of CrMYB68 from *A. thaliana* (*AtMYB68*) serves as a negative regulator (Feng *et al.*, 2004). These data are consistent with the notion that CrMYB68 may negatively regulate the expression of *CrBCH2*. Our results from the SAAB assay and EMSA indicate that CrMYB68 can bind directly to the promoter of *CrBCH2*. Dual luciferase assay indicates that CrMYB68 can also significantly repress the activity of the *CrBCH2* promoter (Fig. 4b,d). Moreover, the transient overexpression of *CrMYB68* in tobacco leaves significantly inhibited the expression of *NbBCH2* (Fig. 5a, b). All these results indicate that CrMYB68 can directly repress the transformation of α- and β-carotene by negatively regulating the expression of *CrBCH2* (Fig. 7).

CrMYB68 regulates ABA biosynthesis

As a crucial hormone in the ripening process, ABA significantly affects carotenoid metabolism in tomato, mango, watermelon, and citrus fruits (Zhang *et al.*, 2009, 2017; Zaharah *et al.*, 2012; Barickman *et al.*, 2014; Wang *et al.*, 2016a,b). Several important genes involved in carotenoid metabolism, such as *PSY3* from maize and *DSM2*, a *BCH* gene from rice, were significantly induced by ABA treatments (Li *et al.*, 2008; Du *et al.*, 2010). These results suggest that ABA, a downstream product of the carotenoid pathway, is a feedback regulator of carotenoid metabolism.

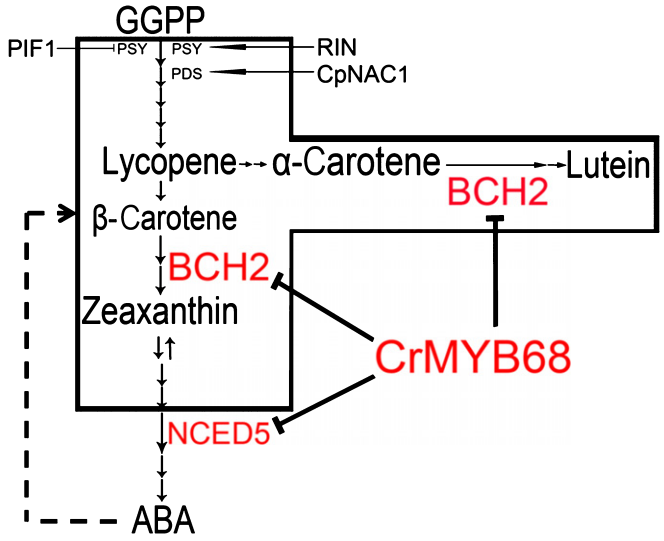

Fig. 7 Model for the transcriptional regulation of carotenoid metabolism by CrMYB68. In addition to phytochrome-interacting factor 1 (PIF1), RIPENING INHIBITOR (RIN) and CpNAC1, which regulate early lycopene biosynthesis, CrMYB68 can significantly regulate carotenoid metabolism by controlling the expression of the genes involved in the metabolism of the α- and β-branch carotenoids. On the one hand, CrMYB68 can affect the transformation of α- and β-carotene by directly repressing the expression of *CrBCH2*. On the other hand, CrNCED5, which catalyzes the transformation of the final carotenoid products of the β-branch, is also regulated by CrMYB68. Moreover, ABA, the downstream product of the CrNCED5 catalyzed reaction, feedback regulates carotenoid metabolism. The details of this regulatory mechanism require further research.

In the present study, we found that ABA was accumulated in parallel with the increase in the CI in WT during the preharvest stage (Fig. 1a,f), which is similar to the case in *Citrus clementina* (Agusti *et al.*, 2007). During the ripening process, the concentration of ABA was lower in MT flavedo than in WT and MT-WT flavedos (Figs 1f, 6e). Moreover, in citrus, the expression of the two genes which encode rate-limiting enzymes in ABA biosynthesis (*CsNCED3* and *CcNCED5*) is induced during the color change in the flavedo of *C. sinensis* (with *CsNCED3* being more important) and *C. clementina* (with *CcNCED5* being more important) during fruit ripening (Agusti *et al.*, 2007). Because Ougan (*C. reticulata* cv *Suavissima*) shows greater similarity to *C. clementina* than to *C. sinensis* (Federici *et al.*, 1998), we infer that *CrNCED5* is probably the rate-limiting enzyme for ABA biosynthesis in the flavedo of WT. In the present study, we found that the expression of *CrNCED5* was significantly lower in MT flavedo than in the flavedos of both WT and MT-WT (Figs 2d, 6f). Moreover, the transient overexpression of *CrNCED5* significantly induced the accumulation of ABA in tobacco leaves (Fig. S5). All these results indicate that the low expression of *CrNCED5* may at least partially explain the low ABA concentration in the flavedo of MT.

As one of the most important genes in ABA biosynthesis, the *NCEDs* gene is a hot topic in ABA metabolism research. Since the function of NCEDs has been thoroughly elucidated, the transcriptional regulation of this gene has become a new focus to illustrate the vital role of this gene in ABA metabolism (Jiang *et al.*, 2012; Jensen *et al.*, 2013; Zong *et al.*, 2016). In the present study, we found that the expression of *CrNCED5* and *CrMYB68* was inversely correlated in the flavedo of MT during fruit development (Fig. 2c,d). Additionally, the SAAB assay and the EMSA demonstrated that CrMYB68 can bind directly to the AC-rich domain (ACCAAA) in the promoter of *CrNCED5* (Fig. 4b). Moreover, the results of the dual luciferase assay indicated that the activity of the *CrNCED5* promoter was significantly repressed by CrMYB68 (Fig. 4d). Furthermore, the transient overexpression of *CrMYB68* inhibited the expression of *NbNCED5* in tobacco leaves (Fig. 5a,b). These results indicate that CrMYB68 can indirectly affect carotenoid metabolism in MT fruits by directly repressing the biosynthesis of ABA. Further studies are needed for a more in-depth understanding of the regulation of carotenoid metabolism by ABA (Fig. 7).

The colors of fruits are highly variable because of the differences in the pigments they accumulate, such as carotenoids, anthocyanins and betalains (Barrett *et al.*, 2010). In recent decades, the MYB family of genes has been demonstrated to directly regulate the biosynthesis of anthocyanins and betalains in different species. Examples of *MYB* genes that regulate the accumulation of anthocyanins include *Production of anthocyanin*

pigments (*PAPs*) in *A. thaliana*, *FaMYB1* in *Fragaria* × *ananasa*, *Ruby* in blood orange, and *PpMYB10.1* in *Prunus persica*. *BvMYB1* regulates the accumulation of betalains in *Beta vulgaris* (Aharoni *et al.*, 2001; Dubos *et al.*, 2010; Butelli *et al.*, 2012; Maier *et al.*, 2013; Hatlestad *et al.*, 2015; Tuan *et al.*, 2015). Carotenoids also contribute to the beautiful colors of fruits and flowers. An R2R3-MYB (*RCP1*) positively regulates the accumulation of carotenoids in *M. lewisii* (Sagawa *et al.*, 2016), although the details of this regulatory mechanism remain unknown. In summary, the clarification of the direct regulatory function of CrMYB68 in the present study not only contributes to the illustration of the transcriptional regulation of carotenoid metabolism, but also further expands our understanding of the roles of MYB TFs in the regulation of pigment metabolism. In nature, pigments play important roles in the appearance and quality of fruits. Because of their high efficiency and effectiveness in the regulation of pigment metabolism, TFs such as CrMYB68 should be thoroughly studied for the genetic breeding programs aimed at producing more beautiful and health-promoting fruits.

Identification of bud mutants is one of the most important approaches for developing valuable fruit cultivars for economically significant fruit crops, such as citrus, grape, apple and persimmon (Shamel & Pomeroy, 1932; Liu *et al.*, 2007; Yamane *et al.*, 2008; Pelsy, 2010). Bud mutants may be caused by point mutations, large deletions, and the insertions of retrotransposons. In natural populations, bud mutants occur at rates ranging from 10^{-5} to 10^{-8} (Shen & Lin, 1985; Yao *et al.*, 2001; Kobayashi *et al.*, 2004; Pelsy, 2010; Butelli *et al.*, 2012). In our case, the bud mutant (MT, Green Ougan) was found in 2000. Then, the orchardist reproduced > 40 000 MT trees in a 17 ha orchard by grafting. In 2013, a revertant branch was found on an MT tree among the *c.* 800 000 branches of the 40 000 MT trees. In the future, whole-genome sequencing of WT, MT, and MT-WT will be used to identify the mutant allele responsible for the phenotypes of MT and the revertant.

Acknowledgements

We thank Dr Masaru Ohme-Takagi (National Institute of Advanced Industrial Science and Technology, Japan) for providing the plasmids 35S-GAL4-fLUC, Dr Shouyi Chen (Institute of Genetics and Developmental Biology, China) for providing the plasmids None and AtUbi3-rLUC, and Dr Wei Zong and Lizhong Xiong (Huazhong Agricultural University) for providing plasmids pM999-35 and 35S:Ghd7–CFP. Moreover, we also thank the research associates at the Center for Protein Research, Huazhong Agricultural University, for technical support. This work was supported by the National Natural Science Foundation of China (no. 31572176, 31330066 and 31521092), the Special Fund for Agro-scientific Research in the Public Interest (no. 201303093), the National Modern Agriculture (Citrus) Technology Systems of China (no. CARS-27), the National Science & Technology Pillar Program of China (2015BAD16B06), and Huazhong Agricultural University Scientific & Technological Self-innovation Foundation. Finally, we thank Prof. Zuoxiong Liu for editing the English language of the manuscript.

Author contributions

F.Z. and Y.C. conceived this project and designed all of the experiments. F.Z., T.L., C.L., Y.W., H.Y., W.Y., L.Z., X.X., M.Z. and R.X. performed the experiments. Jianguo Xu, Y.Z., Juan Xu, Q.X., W.G., R.M.L., Y.C. and X.D. supervised the experiments. F.Z., T.L., L.Z. and H.Y. analyzed the data. F.Z. and Y.C. wrote the article.

References

Agusti J, Zapater M, Iglesias DJ, Cercos M, Tadeo FR, Talon M. 2007. Differential expression of putative 9-cis-epoxycarotenoid dioxygenases and abscisic acid accumulation in water stressed vegetative and reproductive tissues of citrus. *Plant Science* **172**: 85–94.

Aharoni A, De Vos CHR, Wein M, Sun Z, Greco R, Kroon AR, Mol JNM, Oconnell AP. 2001. The strawberry *FaMYB1* transcription factor suppresses anthocyanin and flavonol accumulation in transgenic tobacco. *Plant Journal* **28**: 319–332.

Alos E, Roca M, Iglesias DJ, Minguez-Mosquera MI, Damasceno CMB, Thannhauser TW, Rose JKC, Talon M, Cercos M. 2008. An evaluation of the basis and consequences of a stay-green mutation in the *navel negra* citrus mutant using transcriptomic and proteomic profiling and metabolite analysis. *Plant Physiology* **147**: 1300–1315.

Arango J, Jourdan M, Geoffriau E, Beyer P, Welsch R. 2014. Carotene hydroxylase activity determines the levels of both α-carotene and total carotenoids in orange carrots. *Plant Cell* **26**: 2223–2233.

Bailey TL. 2011. DREME: motif discovery in transcription factor ChIP-seq data. *Bioinformatics* **27**: 1653–1659.

Barickman TC, Kopsell DA, Sams CE. 2014. Abscisic acid increases carotenoid and chlorophyll concentrations in leaves and fruit of two tomato genotypes. *Journal of the American Society for Horticultural Science* **139**: 261–266.

Barrett DM, Beaulieu JC, Shewfelt R. 2010. Color, flavor, texture, and nutritional quality of fresh-cut fruits and vegetables: desirable levels, instrumental and sensory measurement, and the effects of processing. *Critical Reviews in Food Science and Nutrition* **50**: 369–389.

Bustin SA, Benes V, Garson JA, Hellemans J, Huggett JF, Kubista M, Mueller R, Nolan T, Pfaffl MW, Shipley GL. 2009. The MIQE guidelines: minimum information for publication of quantitative Real-Time PCR experiments. *Clinical Chemistry* **55**: 611–622.

Butelli E, Licciardello C, Zhang Y, Liu J, Mackay S, Bailey P, Reforgiato-Recupero G, Martin C. 2012. Retrotransposons control fruit-specific, cold-dependent accumulation of anthocyanins in blood oranges. *Plant Cell* **24**: 1242–1255.

Cazzaniga S, Li ZR, Niyogi KK, Bassi R, Dall'Osto L. 2012. The Arabidopsis *szl1* mutant reveals a critical role of β-carotene in photosystem I photoprotection. *Plant Physiology* **159**: 1745–1758.

Cazzonelli CI. 2011. Carotenoids in nature: insights from plants and beyond. *Functional Plant Biology* **38**: 833–847.

Davuluri GR, Van Tuinen A, Fraser PD, Manfredonia A, Newman R, Burgess D, Brummell DA, King SR, Palys J, Uhlig J. 2005. Fruit-specific RNAi-mediated suppression of *DET1* enhances carotenoid and flavonoid content in tomatoes. *Nature Biotechnology* **23**: 890–895.

Demmigadams B, Adams WW, Logan BA, Verhoeven AS. 1995. Xanthophyll cycle-dependent energy dissipation and flexible photosystem II efficiency in plants acclimated to light stress. *Functional Plant Biology* **22**: 249–260.

Diretto G, Welsch R, Tavazza R, Mourgues F, Pizzichini D, Beyer P, Giuliano G. 2007. Silencing of β-carotene hydroxylase increases total carotenoid and β-carotene levels in potato tubers. *BMC Plant Biology* **7**: 11.

Du H, Wang N, Cui F, Li X, Xiao J, Xiong L. 2010. Characterization of the β-carotene hydroxylase gene *DSM2* conferring drought and oxidative stress resistance by increasing xanthophylls and abscisic acid synthesis in rice. *Plant Physiology* **154**: 1304–1318.

Dubos C, Stracke R, Grotewold E, Weisshaar B, Martin C, Lepiniec L. 2010. MYB transcription factors in *Arabidopsis*. *Trends in Plant Science* **15**: 573–581.

Federici TC, Fang QD, Scora WR, Roose LM. 1998. Phylogenetic relationships within the genus *Citrus* (*Rutaceae*) and related genera as revealed by RFLP and RAPD analysis. *Theoretical and Applied Genetics* **96**: 812–822.

Feng CP, Andreasson E, Maslak A, Mock HP, Mattsson O, Mundy J. 2004. *Arabidopsis MYB68* in development and responses to environmental cues. *Plant Science* **167**: 1099–1107.

Finkelstein R. 2013. Abscisic Acid synthesis and response. *The Arabidopsis Book* **11**: e0166.

Fu CC, Han YC, Fan ZQ, Chen JY, Chen WX, Lu WJ, Kuang JF. 2016. The papaya transcription factor CpNAC1 modulates carotenoid biosynthesis through activating phytoene desaturase genes *CpPDS2/4* during fruit ripening. *Journal of Agricultural and Food Chemistry* **64**: 5454–5463.

Gómez-Maldonado J, Avila C, de la Torre F, Cañas R, Cánovas FM, Campbell MM. 2004. Functional interactions between a glutamine synthetase promoter and MYB proteins. *Plant Journal* **39**: 513–526.

Hatlestad GJ, Akhavan NA, Sunnadeniya RM, Elam L, Cargile S, Hembd A, Gonzalez A, McGrath JM, Lloyd AM. 2015. The beet *Y* locus encodes an anthocyanin MYB-like protein that activates the betalain red pigment pathway. *Nature Genetics* **47**: 92–96.

Hellens RP, Allan AC, Friel EN, Bolitho K, Grafton K, Templeton MD, Karunairetnam S, Gleave AP, Laing WA. 2005. Transient expression vectors for functional genomics, quantification of promoter activity and RNA silencing in plants. *Plant Methods* **1**: 13.

Jensen MK, Lindemose S, de Masi F, Reimer JJ, Nielsen M, Perera V, Workman CT, Turck F, Grant MR, Mundy J *et al.* 2013. ATAF1 transcription factor directly regulates abscisic acid biosynthetic gene *NCED3* in *Arabidopsis thaliana*. *FEBS Open Bio* **3**: 321–327.

Jiang YJ, Liang G, Yu DQ. 2012. Activated expression of WRKY57 confers drought tolerance in *Arabidopsis*. *Molecular Plant* **5**: 1375–1388.

Kato M, Ikoma Y, Matsumoto H, Sugiura M, Hyodo H, Yano M. 2004. Accumulation of carotenoids and expression of carotenoid biosynthetic genes during maturation in citrus fruit. *Plant Physiology* **134**: 824–837.

Kobayashi S, Gotoyamamoto N, Hirochika H. 2004. Retrotransposon-induced mutations in grape skin color. *Science* **304**: 982.

Lee JM, Joung JG, McQuinn R, Chung MY, Fei ZJ, Tieman D, Klee H, Giovannoni J. 2012. Combined transcriptome, genetic diversity and metabolite profiling in tomato fruit reveals that the ethylene response factor *SlERF6* plays an important role in ripening and carotenoid accumulation. *Plant Journal* **70**: 191–204.

Lewinsohn E, Sitrit Y, Bar E, Azulay Y, Ibdah M, Meir A, Yosef E, Zamir D, Tadmor Y. 2005. Not just colors-carotenoid degradation as a link between pigmentation and aroma in tomato and watermelon fruit. *Trends in Food Science and Technology* **16**: 407–415.

Li F, Vallabhaneni R, Wurtzel ET. 2008. *PSY3*, a new member of the phytoene synthase gene family conserved in the Poaceae and regulator of abiotic stress-induced root carotenogenesis. *Plant Physiology* **146**: 1333–1345.

Liu C, Long J, Zhu K, Liu L, Yang W, Zhang H, Li L, Xu Q, Deng X. 2016. Characterization of a citrus R2R3-MYB transcription factor that regulates the flavonol and hydroxycinnamic acid biosynthesis. *Scientific Reports* **6**: 25352.

Liu G, Ren G, Guirgis A, Thornburg RW. 2009. The MYB305 transcription factor regulates expression of nectarin genes in the ornamental tobacco floral nectary. *Plant Cell* **21**: 2672–2687.

Liu D, Shi L, Han C, Yu J, Li D, Zhang Y. 2012. Validation of reference genes for gene expression studies in virus-infected *Nicotiana benthamiana* using quantitative real-time PCR. *PLoS ONE* **7**: e46451.

Liu C, Wang X, Xu Y, Deng X, Xu Q. 2014. Genome-wide analysis of the R2R3-MYB transcription factor gene family in sweet orange (*Citrus sinensis*). *Molecular Biology Reports* **41**: 6769–6785.

Liu Q, Xu J, Liu Y, Zhao X, Deng X, Guo L, Gu J. 2007. A novel bud mutation that confers abnormal patterns of lycopene accumulation in sweet orange fruit (*Citrus sinensis* L. Osbeck). *Journal of Experimental Botany* **58**: 4161–4171.

Luo T, Xu K, Luo Y, Chen J, Sheng L, Wang J, Han J, Zeng Y, Xu J, Chen J. 2015. Distinct carotenoid and flavonoid accumulation in a spontaneous mutant of ponkan (*Citrus reticulata* Blanco) results in yellowish fruit and enhanced postharvest resistance. *Journal of Agricultural and Food Chemistry* **63**: 8601–8614.

Ma Q, Ding Y, Chang J, Sun X, Zhang L, Wei Q, Cheng Y, Chen L, Xu J, Deng X. 2014. Comprehensive insights on how 2,4-dichlorophenoxyacetic acid retards senescence in post-harvest citrus fruits using transcriptomic and proteomic approaches. *Journal of Experimental Botany* **65**: 61–74.

Ma G, Zhang L, Yungyuen W, Tsukamoto I, Iijima N, Oikawa M, Yamawaki K, Yahata M, Kato M. 2016. Expression and functional analysis of citrus carotene hydroxylases: unravelling the xanthophyll biosynthesis in citrus fruits. *BMC Plant Biology* **16**: 148.

Maier A, Schrader A, Kokkelink L, Falke C, Welter B, Iniesto E, Rubio V, Uhrig JF, Hulskamp M, Hoecker U. 2013. Light and the E3 ubiquitin ligase COP1/SPA control the protein stability of the MYB transcription factors PAP1 and PAP2 involved in anthocyanin accumulation in Arabidopsis. *Plant Journal* **74**: 638–651.

Martel C, Vrebalov J, Tafelmeyer P, Giovannoni JJ. 2011. The tomato MADS-box transcription factor RIPENING INHIBITOR interacts with promoters involved in numerous ripening processes in a COLORLESS NONRIPENING-dependent manner. *Plant Physiology* **157**: 1568–1579.

Obenland D, Sievert J, Arpaia ML. 2011. Evaluation of a rapid, potable and easy-to-use device to measure acidity in citrus. *Citrograph* May/June: 41–43.

Pelsy F. 2010. Molecular and cellular mechanisms of diversity within grapevine varieties. *Heredity* **104**: 331–340.

Rodrigo MJ, Alquezar B, Alos E, Lado J, Zacarias L. 2013. Biochemical bases and molecular regulation of pigmentation in the peel of *Citrus* fruit. *Scientia Horticulturae* **163**: 46–62.

Rodrigo MJ, Marcos JF, Alferez F, Mallent MD, Zacarias L. 2003. Characterization of Pinalate, a novel *Citrus sinensis* mutant with a fruit-specific alteration that results in yellow pigmentation and decreased ABA content. *Journal of Experimental Botany* **54**: 727–738.

Rodrigo MJ, Marcos JF, Zacarias L. 2004. Biochemical and molecular analysis of carotenoid biosynthesis in flavedo of orange (*Citrus sinensis* L.) during fruit development and maturation. *Journal of Agricultural and Food Chemistry* **52**: 6724–6731.

Sagawa JM, Stanley LE, LaFountain AM, Frank HA, Liu C, Yuan YW. 2016. An R2R3-MYB transcription factor regulates carotenoid pigmentation in *Mimulus lewisii* flowers. *New Phytologist* **209**: 1049–1057.

Searle GF, Wessels JS. 1978. Role of β-carotene in the reaction centres of photosystems I and II of spinach chloroplasts prepared in non-polar solvents. *Biochimica et Biophysica Acta* **504**: 84–89.

Shamel AD, Pomeroy CS. 1932. BUD VARIATION IN APPLES a study of the rôle of bud mutation in deciduous fruit improvement. *Journal of Heredity* **23**: 213–221.

Shen D, Lin B. 1985. *Genetics of horticultural plant.* Beijing, China: Agriculture Press.

Shen C, Zhang D, Guan Z, Liu Y, Yang Z, Yang Y, Wang X, Wang Q, Zhang Q, Fan S *et al.* 2016. Structural basis for specific single-stranded RNA recognition by designer pentatricopeptide repeat proteins. *Nature Communications* **7**: 11285.

Shewmaker CK, Sheehy JA, Daley M, Colburn S, Ke DY. 1999. Seed-specific overexpression of phytoene synthase: increase in carotenoids and other metabolic effects. *Plant Journal* **20**: 401–412.

Sun Z, Gantt E, Cunningham FX Jr. 1996. Cloning and functional analysis of the β-carotene hydroxylase of *Arabidopsis thaliana*. *Journal of Biological Chemistry* **271**: 24349–24352.

Tamura K, Peterson D, Peterson N, Stecher G, Nei M, Kumar S. 2011. MEGA5: Molecular Evolutionary Genetics Analysis using maximum likelihood, evolutionary distance, and maximum parsimony methods. *Molecular Biology and Evolution* **28**: 2731–2739.

Telfer A. 2005. Too much light? How β-carotene protects the photosystem II reaction centre. *Photochemical & Photobiological Sciences* **4**: 950–956.

Tian L, Musetti V, Kim J, Magallaneslundback M, Dellapenna D. 2004. The Arabidopsis *LUT1* locus encodes a member of the cytochrome P450 family that is required for carotenoid ε-ring hydroxylation activity. *Proceedings of the National Academy of Sciences, USA* **101**: 402–407.

Toledoortiz G, Huq E, Rodriguezconcepcion M. 2010. Direct regulation of phytoene synthase gene expression and carotenoid biosynthesis by phytochrome-interacting factors. *Proceedings of the National Academy of Sciences, USA* **107**: 11626–11631.

Tuan PA, Bai SL, Yaegaki H, Tamura T, Hihara S, Moriguchi T, Oda K. 2015. The crucial role of *PpMYB10.1* in anthocyanin accumulation in peach and relationships between its allelic type and skin color phenotype. *BMC Plant Biology* **15**: 280.

Wang Y, Li B, Du M, Eneji AE, Wang B, Duan L, Li Z, Tian X. 2012. Mechanism of phytohormone involvement in feedback regulation of cotton leaf senescence induced by potassium deficiency. *Journal of Experimental Botany* **63**: 5887–5901.

Wang J, Sun L, Xie L, He Y, Luo T, Sheng L, Luo Y, Zeng Y, Xu J, Deng X *et al.* 2016a. Regulation of cuticle formation during fruit development and ripening in 'Newhall' navel orange (*Citrus sinensis* Osbeck) revealed by transcriptomic and metabolomic profiling. *Plant Science* **243**: 131–144.

Wang XH, Yin W, Wu JX, Chai LJ, Yi HL. 2016b. Effects of exogenous abscisic acid on the expression of citrus fruit ripening-related genes and fruit ripening. *Scientia Horticulturae* **201**: 175–183.

Weiler EW, Jourdan P, Conrad WR. 1981. Levels of indole-3-acetic acid in intact and decapitated coleoptiles as determined by a specific and highly sensitive solid-phase enzyme immunoassay. *Planta* **153**: 561–571.

Weng L, Zhao F, Li R, Xu C, Chen K, Xiao H. 2015. The zinc finger transcription factor *SlZFP2* negatively regulates abscisic acid biosynthesis and fruit ripening in tomato. *Plant Physiology* **167**: 931–949.

Xu Q, Chen L, Ruan X, Chen D, Zhu A, Chen C, Bertrand D, Jiao W, Hao B, Lyon MP. 2013. The draft genome of sweet orange (*Citrus sinensis*). *Nature Genetics* **45**: 59–66.

Xu Q, Yu K, Zhu A, Ye J, Liu Q, Zhang J, Deng X. 2009. Comparative transcripts profiling reveals new insight into molecular processes regulating lycopene accumulation in a sweet orange (*Citrus sinensis*) red-flesh mutant. *BMC Genomics* **10**: 540.

Yamane H, Ichiki M, Tao R, Esumi T, Yonemori K, Niikawa T, Motosugi H. 2008. Growth characteristics of a small-fruit dwarf mutant arising from bud sport mutation in Japanese persimmon (*Diospyros kaki* Thunb.). *HortScience* **43**: 1726–1730.

Yan JX, Wait R, Berkelman T, Harry RA, Westbrook JA, Wheeler CH, Dunn MJ. 2000. A modified silver staining protocol for visualization of proteins compatible with matrix-assisted laser desorption/ionization and electrospray ionization-mass spectrometry. *Electrophoresis* **21**: 3666–3672.

Yang J, Zhang J, Wang Z, Zhu Q, Wang W. 2001. Hormonal changes in the grains of rice subjected to water stress during grain filling. *Plant Physiology* **127**: 315–323.

Yao J, Dong Y, Morris BAM. 2001. Parthenocarpic apple fruit production conferred by transposon insertion mutations in a MADS-box transcription factor. *Proceedings of the National Academy of Sciences, USA* **98**: 1306–1311.

Yin XR, Xie XL, Xia XJ, Yu JQ, Ferguson IB, Giovannoni JJ, Chen KS. 2016. Involvement of an ethylene response factor in chlorophyll degradation during citrus fruit degreening. *Plant Journal* **86**: 403–412.

Zaharah SS, Singh Z, Symons GM, Reid JB. 2012. Role of brassinosteroids, ethylene, abscisic acid, and indole-3-acetic acid in mango fruit ripening. *Journal of Plant Growth Regulation* **31**: 363–372.

Zechmeister L, Polgar A. 1941. The carotenoid and provitamin a content of the watermelon. *Journal of Biological Chemistry* **139**: 193–198.

Zhang J, Guo S, Ren Y, Zhang H, Gong G, Zhou M, Wang G, Zong M, He H, Liu F *et al.* 2017. High-level expression of a novel chromoplast phosphate transporter ClPHT4;2 is required for flesh color development in watermelon. *New Phytologist* **213**: 1208–1221.

Zhang B, Liu C, Wang Y, Yao X, Wang F, Wu J, King GJ, Liu K. 2015. Disruption of a *CAROTENOID CLEAVAGE DIOXYGENASE 4* gene converts flower colour from white to yellow in *Brassica* species. *New Phytologist* **206**: 1513–1526.

Zhang M, Yuan B, Leng P. 2009. The role of ABA in triggering ethylene biosynthesis and ripening of tomato fruit. *Journal of Experimental Botany* **60**: 1579–1588.

Zhu F, Chen J, Xiao X, Zhang M, Yun Z, Zeng Y, Xu J, Cheng Y, Deng X. 2016. Salicylic acid treatment reduces the rot of postharvest citrus fruit by inducing the accumulation of H_2O_2, primary metabolites and lipophilic polymethoxylated flavones. *Food Chemistry* **207**: 68–74.

Zong W, Tang N, Yang J, Peng L, Ma S, Xu Y, Li G, Xiong L. 2016. Feedback regulation of ABA signaling and biosynthesis by a bZIP transcription factor targets drought-resistance-related genes. *Plant Physiology* **171**: 2810–2825.

Supporting Information

Additional Supporting Information may be found online in the Supporting Information tab for this article:

Fig. S1 Differences in the qualitative properties (total soluble solid, titratable acid, firmness, and rotting rate) and the content of β-cryptoxanthin, 9-cis-vioxanthin, and lutein in the flavedo of the two genotypes in 2013.

Fig. S2 ABA content of the samples harvested in 2011.

Fig. S3 Numbers of differentially expressed genes during different stages of development in the two genotypes.

Fig. S4 Cluster heat map based on the expression of genes involved in carotenoid and ABA metabolism obtained from the Digital Gene Expression Profiling results.

Fig. S5 Phenotype induced by the transient overexpression of *CrBCH2* and *CrNCED5*.

Fig. S6 Phylogenetic analysis of CrMYB68 and *Arabidopsis thaliana* MYB proteins.

Fig. S7 Alignment of the amino acid sequences of CrMYB68, AtMYB6, and AtMYB4.

Table S1 Primers used in this study

Table S2 Name, synonym, and TAIR ID of 126 MYBs from *Arabidopsis thaliana*

Table S3 Transcriptome data of MT and WT

Table S4 Sequences of *CrNCED5*, *CrBCH2*, and *CrMYB68* in the two genotypes

Table S5 Peptides of CrMYB68 identified by the MALDI-TOF/TOF MS method

Table S6 SAAB results of CrMYB68

Please note: Wiley Blackwell are not responsible for the content or functionality of any Supporting Information supplied by the authors. Any queries (other than missing material) should be directed to the *New Phytologist* Central Office.